The Astrophysical Journal, 632:1001–1007, 2005 October 20

FIREBALLS FROM QUARK STARS IN THE COLOR-FLAVOR LOCKED PHASE: APPLICATION TO GAMMA-RAY BURSTS

Rachid Ouyed,[1] Ralf Rapp,[2] and Carsten Vogt[3]
Received 2005 March 16; accepted 2005 June 28

ABSTRACT

Recent studies of photon generation mechanisms in the color-superconducting color-flavor locked (CFL) phase of dense quark matter have found γ-ray emissivities in excess of $\sim 10^{50}$ ergs cm^{-3} s^{-1} for temperatures in the 10–30 MeV range. We suggest that this property can trigger γ-ray bursts (GRBs) and associated fireballs at the surface of hypothetical hot (newly born) quark stars with an energy release of up to 10^{48}–10^{50} ergs within a fraction of a millisecond. If surrounded by an accretion disk following its formation, the star's bursting activity can last from tens of milliseconds to hundreds of seconds, releasing up to 10^{52} ergs in total energy. We discuss typical features of observed GRBs within our model and explain how quark stars in the CFL phase might constitute natural candidates for corresponding inner engines.

Subject headings: dense matter — gamma rays: bursts — stars: evolution — stars: interiors

1. INTRODUCTION

Nuclear matter at high density and low temperature (T) is expected to exhibit color-superconductivity (CSC), induced by quark pairing and condensation at the Fermi surface, with energy gaps $\Delta \simeq 100$ MeV (Rapp et al. 1998; Alford et al. 1998) and associated critical temperatures $T_c \simeq 0.6\Delta$, above which thermal fluctuations destroy the condensate (for a review, see, e.g., Rajagopal & Wilczek 2001). The experimental relevance of such matter mostly pertains to astrophysical objects, in particular compact stars. Besides its impact on the equation of state (Lugones & Horvath 2002; Alford & Reddy 2003), CSC could affect the emission spectrum of compact stars as encoded in its electroweak properties (Jaikumar et al. 2002; Reddy et al. 2003; Vogt et al. 2004). If CSC extends to the surface of a hypothetical quark star, pulsed photon emission has been suggested as a mechanism for a fireball in the γ-ray burst (GRB) context for the two-flavor superconductor (2SC) in Ouyed & Sannino (2002).[4] Whereas at moderate densities (and $T = 0$) the existence of the 2SC is still under debate (Alford & Rajagopal, 2002; Buballa et al. 2004)—it could be superseeded by, e.g., crystalline phases (Alford et al. 2001; Rapp et al. 2001)—the color-flavor locked (CFL) phase is the favored ground state at sufficiently high density (Alford et al. 1999). In CFL matter all three quark flavors (up, down, and strange) have a mass that is negligible compared to the (quark) chemical potential, μ_q, so that they participate equally in the color condensation, breaking the full (local) color symmetry and one (global) $SU(3)$ chiral symmetry. Therefore, the zero-temperature CFL phase is electrically neutral without electrons, it is colorless, and its low-lying excitations are characterized by $8 + 1$ Goldstone bosons (due to chiral and baryon number symmetry breaking).

In previous work (Vogt et al. 2004, hereafter VRO04), we have explored photon emission and absorption mechanisms in the CFL phase. Based on the Goldstone boson excitations ("generalized pions") of the broken chiral symmetry, we have employed a hidden local symmetry formalism including vector mesons ("generalized ρ mesons") to assess photon production rates and mean free paths at temperatures suitable for CFL. We have found that above $T \simeq 5$–10 MeV, the emissivities from pion annihilation, $\pi^+\pi^- \rightarrow \gamma\gamma$ and $\pi^+\pi^- \rightarrow \gamma$ (rendered possible due to an in-medium pion dispersion relation), dominate over those from conventional electromagnetic annihilation, $e^+e^- \rightarrow \gamma\gamma$. Given the very small photon mean free path at the temperatures of interest, $T = 10$–30 MeV (see Fig. 3 in VRO04), emission and absorption are in equilibrium and reflect the surface temperature of the star with a flux corresponding to that of a blackbody emitter. Therefore, the pertinent cooling will largely depend on how efficiently heat conducted by the Goldstone bosons from the interior can be emitted from the surface in the form of the thermalized photons. The objective of the present article is to (1) investigate the astrophysical consequences of such photon production mechanisms[5] for the early cooling history of hot CFL stars (§ 2) and (2) evaluate whether the resulting fireballs can drive/power GRBs (§ 3). Conclusions are given in § 4.

2. EARLY COOLING OF COLOR-FLAVOR LOCKED STARS

2.1. *Plasma Photon Attenuation*

The surface emissivity of photons with energies below $\hbar\omega_p \simeq 23$ MeV (where ω_p is the electromagnetic plasma frequency) is strongly suppressed (Alcock et al. 1986; Chmaj et al. 1991; Usov 2001). As shown in VRO04, average photon energies in CFL matter at temperature T are $\sim 3T$. Therefore, as soon as the

[1] Department of Physics and Astronomy, University of Calgary, 2500 University Drive, NW, Calgary, AB T2N 1N4, Canada; ouyed@phas.ucalgary.ca.
[2] Cyclotron Institute and Physics Department, Texas A&M University, College Station, TX 77843-3366.
[3] Nordic Institute for Theoretical Physics, Blegdamsvej 17, DK-2100 Copenhagen, Denmark.

[4] In the 2SC phase, up and down quarks pair into a color antitriplet, leaving the quarks of the remaining color unpaired, with five of the eight gluons acquiring a mass. The three massless gluons possibly bind into light glueballs subject to fast decays into photons (Ouyed & Sannino 2001).

[5] We note that our study is different from those involving the e^+e^- emission above the surface of CFL stars (see, e.g., Page & Usov 2002 and references therein). The latter scenarios reside on the fact that the color-superconductive matter of the star carries a charge so that an e^- abundance can build up, thereby generating a critical electric field that in turn produces and emits e^+e^- pairs and photons. This is quite different from our model, which is based on photon generation inside the star with negligible (e^+e^-) emission.

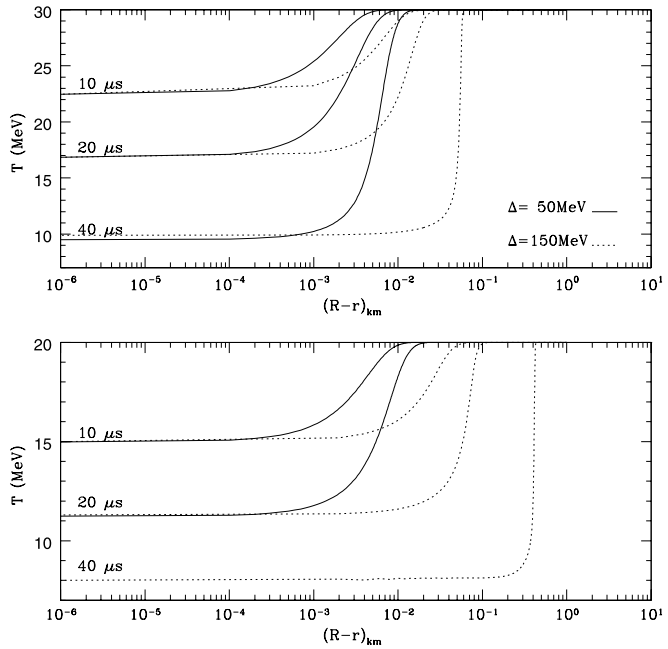

FIG. 1.—Radial temperature profiles of CFL stars of radius R according to solutions of the diffusion eq. (1) (where r is the distance to the star's center) for two different gaps, $\Delta = 50$ MeV (*solid lines*) and 150 MeV (*dotted lines*) and initial temperatures $T_0 = 30$ MeV (*top*) and 20 MeV (*bottom*). In the bottom panel, the $\Delta = 50$ MeV case cools to $T_a = 7.7$ MeV (lower limit of the plots) in less than 40 μs.

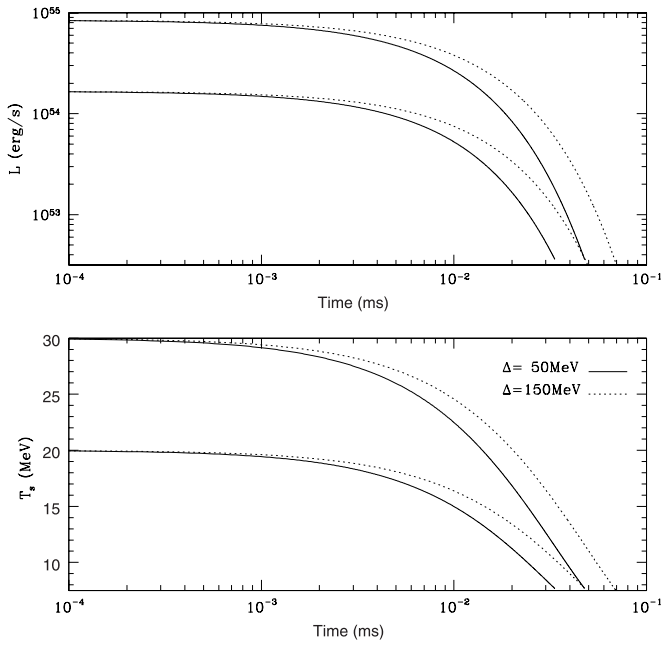

FIG. 2.—Time dependence of photon luminosity (*top*) and surface temperature (*bottom*) of a CFL star for two initial temperatures, $T_0 = 20$ and 30 MeV (*lower and upper pairs of lines, respectively*). Solid lines are for $\Delta = 50$ MeV, and dotted lines are for $\Delta = 150$ MeV.

surface temperature of the star cools below $T_a = \hbar\omega_p/3 \simeq 7.7$ MeV, we consider the photon emissivity to be shut off ("attenuated"); i.e., the photon emission only lasts as long as the star cools from its initial temperature T_0 to T_a. With this in mind, we proceed to study the thermal evolution of the star.

2.2. *Heat Transfer and Thermal Evolution*

We describe the thermal evolution by a diffusion equation,

$$c_v \frac{\partial T}{\partial t} = \frac{1}{r^2}\frac{\partial}{\partial r}\left(r^2 \kappa \frac{\partial T}{\partial r}\right), \tag{1}$$

where c_v and κ are the specific heat and thermal conductivity of the star matter, respectively. In the CFL phase, these are dominated by massless Goldstone bosons, as evaluated in Jaikumar et al. (2002),

$$c_v = \frac{2\sqrt{3}\pi^2}{5} T^3 = 7.8 \times 10^{16} T_{\rm MeV}^3 \text{ ergs cm}^{-3} \text{ K}^{-1}, \tag{2}$$

and in Shovkovy & Ellis (2002),

$$\kappa = 1.2 \times 10^{27} T_{\rm MeV}^3 \lambda_{\rm GB} \text{ ergs cm}^{-1} \text{ s}^{-1} \text{ K}^{-1}, \tag{3}$$

with a Goldstone boson mean free path (in centimeters in eq. [3])

$$\lambda_{\rm GB}(T) = \frac{4(21 - 8\ln 2)}{15\sqrt{2}\pi T_{\rm MeV}} \exp\left(\sqrt{\frac{3}{2}}\frac{\Delta_{\rm MeV}}{T_{\rm MeV}}\right) \text{ cm}. \tag{4}$$

Effects of a crust have been ignored in the present study of the star's cooling history (see discussion in § 3.4).

In dimensionless units, the diffusion equation becomes

$$\frac{\partial \tilde{T}^4}{\partial \tau} = \frac{\alpha}{\tilde{r}^2}\frac{\partial}{\partial \tilde{r}}\left(\tilde{\lambda}_{\rm GB}\tilde{r}^2 \frac{\partial \tilde{T}^4}{\partial \tilde{r}}\right), \tag{5}$$

with $\tilde{r} = r/R\tilde{T} = T/T_0\tau = t/(R/c)$, $\tilde{\lambda}_{\rm GB} = \lambda_{\rm GB}/R$, and a numerical coefficient $\alpha = 0.512$, where c is the speed of light. As an initial condition we assume that the temperature of the star at $\tau = 0$ is uniform, $\tilde{T}(\tau = 0) = \tilde{T}_0$. We further must impose boundary conditions for the temperature gradient in terms of the heat flux, $F(\tilde{r}) = -\tilde{\lambda}_{\rm GB}\left(\partial\tilde{T}/\partial\tilde{r}\right)$, at the center and the surface of the star, $F(\tilde{r} = 0) = 0$ and $F(\tilde{r} = 1) = \tilde{T}^4$. Due to the large opacity, we expect that the photons are thermalized on leaving the star. Thus, we assume blackbody radiation to be a good approximation (supported by VRO04). The energy flux per unit time through a spherical shell at a radius $\tilde{r}$ is evolved by taking into account the gradient of temperature on both sides of the shell. For the outermost shell, the flux exits the star via thermal photons, implying that the cooling curves result from photon emission only.

Numerical solutions to equation (5), using a finite-difference method, are summarized in Figures 1 and 2 for a quark star of radius $R = 10$ km. Figure 1 shows the temperature versus distance from the star's surface, $R - r$, indicating that T drops to T_a in less than 0.1 ms over a shell of thickness less than $\sim$1 km. Neglecting heat transport, the cooling timescale may be roughly estimated from $c_v(\partial T/\partial t) = -\epsilon = -L/\Delta V$ (where $\Delta V = 4\pi R^2 \Delta R$ is the volume of the cooling shell of thickness ΔR). Assuming a blackbody luminosity, $L = 4\pi R^2 \sigma T^4$, one finds $t_{\rm cool} \simeq (0.1 \text{ ms})\Delta R_{\rm km}(\Delta T/T)$ ($\Delta T = T_0 - T_a$), approximately reflecting the numerical results. Note that our estimate improves toward small T and large Δ for which $\lambda_{\rm GB}$ is larger, so that neglecting the delay time due to heat transport (eq. [1]) is better justified; e.g., for $T_0 = 20$ MeV and $\Delta = 150$ MeV (in which case $\lambda_{\rm GB} = 10^{-2}$ km, reaching 1 km at $T \simeq 15$ MeV), $\Delta R_{\rm km} \simeq 1$

(Fig. 1, *bottom*), whereas with $(\Delta T/T) \simeq 1$ one recovers $t_{\rm cool} \simeq 0.1$ ms, consistent with the bottom panel of Figure 2.

For identical T_0, a larger gap implies cooling deeper in the star but slower in terms of the reduction in surface temperature (cf. Fig. 2). Again, this follows from the larger $\lambda_{\rm GB}$, for which heat emerges from deeper in the star and thus provides a larger energy reservoir.

When increasing the initial temperature, T_0, from 20 to 30 MeV, the surface cooling does not change radically. The main difference is that the cooling of the bulk sets in earlier, so that the temperature gradient between surface and bulk is washed out in a shorter time.

We recall that contributions from neutrino (ν) emission are not included in our analysis. By assuming uniform star density and temperature as our initial state, the consequences as shown in VRO04 are that (1) ν emission from the surface is usually negligible in comparison to photon emission in the temperature region we are considering (see § 3.4 in VRO04 for more details) and (2) ν emission from the bulk will set in once the neutrino mean free path becomes comparable to the star radius, which is expected to occur for temperatures below ~5 MeV (Reddy et al. 2003); above that temperature, the neutrinos are essentially trapped inside the star. This point is further discussed in § 4.

We also note that photons will be redshifted as they stream outward due to the star's gravitational potential. First-order general relativity effects on the emissivities can be introduced through redshift factors expressed in terms of the star's mass and radius. We estimate the pertinent redshift reduction to be of the order of 10% (see Frolov & Lee 2005 for a recent analysis). While the gravitational redshift will degrade the total energy emitted, it should not affect the qualitative features of our results.

3. APPLICATION TO GAMMA-RAY BURSTS

The total energy released during cooling is computed from Figure 2 as $E_{\rm tot} = \int L_\gamma\, dt$. Thus, a CFL star with an initial temperature of 10–30 MeV can release on average 10^{48}–10^{50} ergs within ~0.1 ms as it cools to T_a. We have at hand an engine that could be driving observed GRBs.

3.1. *Accretion Disk and Temporal Variability*

Our main idea for the following is that the input energy to the engine is provided by infalling matter from an accretion disk. The energy released by the hot CFL star translates into $(0.01$–$1)M_\odot c^2\ {\rm s}^{-1}$ in accretion energy. These values are reminiscent of hyperaccreting disks (Popham et al. 1999), suggesting that if the latter is indeed formed around a CFL star it could reheat the surface of the star via accretion, keeping the engine active for a much longer time and providing higher energies as compared to collapse events only. More precisely, the total available energy is related to the disk mass, $M_{\rm disk}$, by

$$E_T \simeq \eta M_{\rm disk} c^2 + \frac{M_{\rm disk}}{m_{\rm H}} \Delta E_B, \qquad (6)$$

where the first term accounts for the release in gravitational binding energy of the accreted matter, with $\eta \sim 0.1$ (e.g., Frank et al. 1992). The second term represents the binding energy released in the conversion from nuclear to CFL matter (ΔE_B per nucleon). It is presumably emitted via neutrinos (Glendenning 1997) so that $E_T \simeq \eta M_{\rm disk} c^2$ remains available for photon production.

We are modeling the effects of the accreted material on the CFL star in a very simplistic approach, as a random increase of the CFL surface temperature T_s (heating) to a value $T_{\rm peak}$ with a uniform distribution between the lower limit, $T_a \simeq 7.7$ MeV, and an upper limit, $T_{\rm max} = 15$–30 MeV. This roughly corresponds to expected average disk temperatures up to $T_{\rm disk} \simeq 15$ MeV or so (Popham et al. 1999); we neglect cooling processes during accretion. Note that for accreted material with temperature below T_a, there is no bursting and the engine remains shut off until further accretion drives T_s above T_a. In these cases the accretion proceeds for longer than the average accretion timescale.

For the time intervals of accretion, $\Delta t_{\rm accr}$, we assume the free-fall time for a hyperaccreting disk as the relevant scale, $t_{\rm ff} = 1/(4\pi G \rho_{\rm disk})^{1/2} \simeq 1$ ms, where $\rho_{\rm disk} \simeq 10^{12}$ g cm^{-3} is the accretion disk density and G is the gravitational constant. The accretion time intervals are sampled stochastically between 1 and 10 ms. The timescale, Δt_γ, of the subsequent GRB (cooling) follows from the diffusion equation (5) as the time it takes to cool the surface to T_a. During this time the accretion energy is transformed to photon energy, which in a simple form can be written as $L_\gamma \Delta t_\gamma = \eta \dot{M}_{\rm disk} c^2 \Delta t_{\rm accr}$. Thus, each event (reheating and cooling) lasts for $\Delta t_{\rm event} = \Delta t_{\rm accr} + \Delta t_\gamma$, for given Δ and $T_{\rm peak}$ (we set $\Delta = 50$ MeV). Consequently, each episode lasts for a few milliseconds, consisting of a linear increase of T_s to $T_{\rm peak}$ followed by a rather sharp decrease to T_a.

For a given disk mass (see § 3.5), the simulation is carried out until the total available energy, $E_T \simeq 0.1 M_{\rm disk} c^2$ (eq. [6]), is consumed. The resulting variability (displayed in Figs. 3 and 4 for $E_T = 0.001 M_\odot c^2$ and $0.01 M_\odot c^2$ and typical time resolutions of GRB detectors) shares interesting similarities to those observed in GRB data.[6] Note that our spectra correspond to the activity directly at the engine, while the GRB curves represent emission beyond the transparency radius (see, e.g., Piran 2000). Nevertheless, the engine activity should reflect the variability at large distances.

3.2. *Total Duration*

Our simulations of the accretion suggest engine activities varying from milliseconds to hundreds of seconds depending on $M_{\rm disk}$ and $T_{\rm max}$ (Figs. 3 and 4). The average duration can be estimated as $t_{\rm dur} \simeq \Delta \bar{t}_{\rm accr}(E_T/\bar{E}_\gamma)$ with average burst energy and accretion timescale $\bar{E}_\gamma \simeq 10^{49}$ ergs and $\Delta \bar{t}_{\rm accr} \simeq 5$ ms, respectively. One obtains $t_{\rm dur} \simeq 10$ s for a CFL star surrounded by a 0.1 $M_\odot$ disk. For this disk mass (corresponding to $E_T = 0.01 M_\odot c^2$), the engine activity can last for hundreds of seconds if $T_{\rm max}$ is sufficiently low (e.g., 15 MeV, as in Fig. 5). In general, for a given $M_{\rm disk}$, smaller $T_{\rm max}$ imply smaller average energies released per episode (i.e., smaller accretion rates) and thus longer lifetimes.

We also note that the variability observed in the first few seconds of the $E_T = 0.01 M_\odot c^2$ simulations is very similar to that in the $E_T = 0.001 M_\odot c^2$ case, which lasts for ~2 s (recall Figs. 3 and 4). In addition, the variability seen in the first few seconds of a $E_T = 0.1 M_\odot c^2$ simulation (not shown here) bears many similarities to the $E_T = 0.01 M_\odot c^2$ case. This "self-similar" behavior occurs because the duration is controlled by accretion timescales $\Delta t_{\rm accr} > \Delta t_\gamma$, in connection with the stochastic accretion process whose main effect is to spread the events (peaks) randomly in time.

[6] See, e.g., http://www.batse.msfc.nasa.gov/batse/grb/lightcurve.

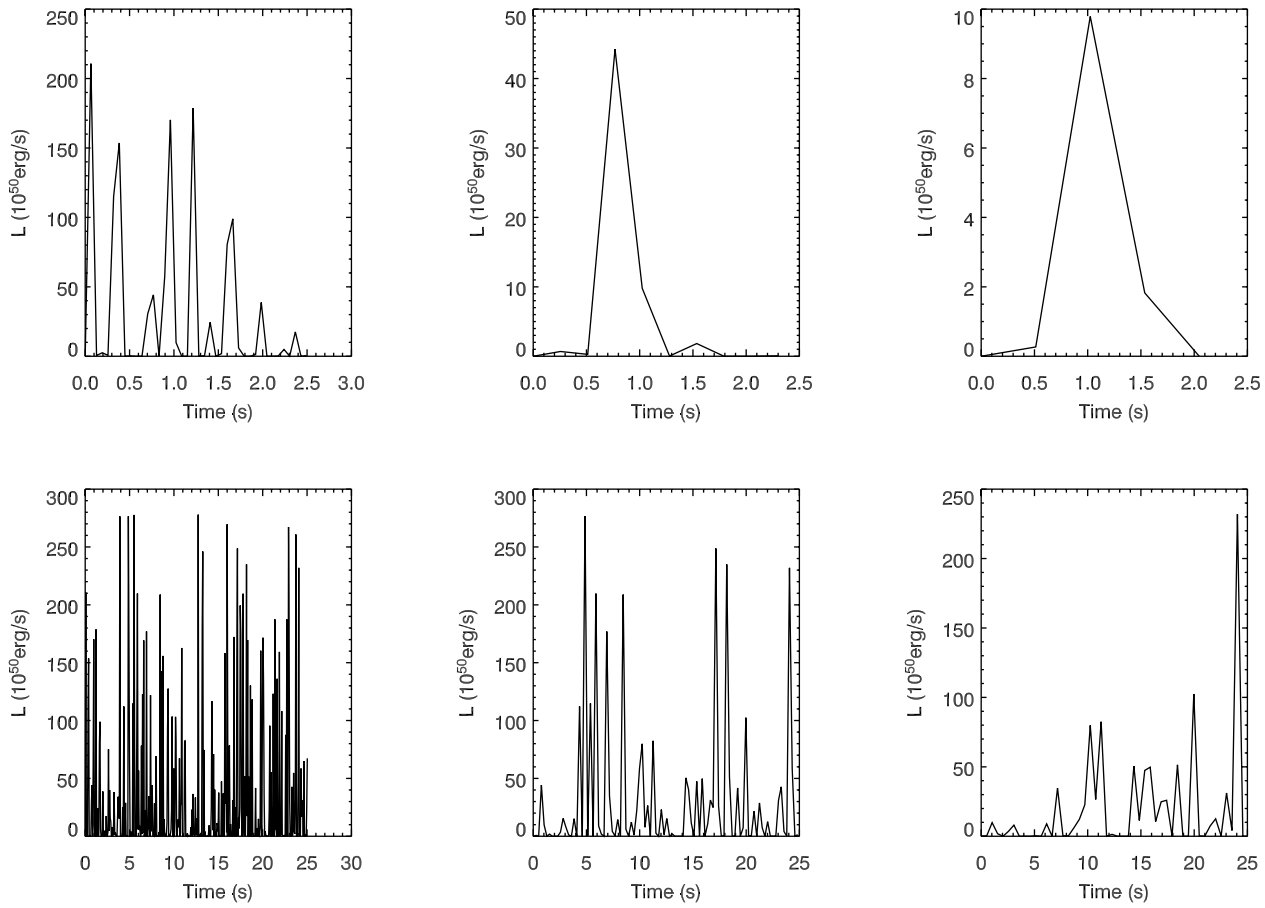

FIG. 3.—Model results for the effects of a hyperaccreting disk on the star luminosity; shown is the GRB emission vs. time for three different time resolutions (64, 256, and 512 ms, *from left to right*) representative of GRB detectors (see http://www.batse.msfc.nasa.gov/batse/grb/lightcurve/). The top panels are for a total accreted energy $E_T = 0.001 M_\odot c^2$, and the bottom panels are for $E_T = 0.01 M_\odot c^2$, with $T_{\max} = 30$ MeV.

3.3. *Total Energy*

In our model up to 10% of $M_{\rm disk}c^2$ can be transformed into fireball energy; e.g., if an accretion disk with mass 0.1 $M_\odot$ surrounds a CFL star following its formation (see § 3.5), up to 10^{52} ergs of energy can be released in γ-rays. Larger disks lead to higher energy release, but in this case the star is likely to become a black hole in the process.

3.4. *Baryon Loading and Beaming*

The intense, localized (source size <100 km), and brief explosion implied by the observed GRB fluxes suggest the formation of a e^+e^--photon fireball. Furthermore, most of the spectral energy in GRBs is observed at $\geq$0.5 MeV, so the optical depth for $\gamma\gamma \rightarrow e^+e^-$ processes is very large. Any photon generated above 0.511 MeV will be degraded to below 0.511 MeV via the $\gamma\gamma \rightarrow e^+e^-$ process. This is the so-called compactness problem leading to a thermalized fireball (Ruderman 1975) unlike the optically thin spectra observed in GRBs.

The compactness problem can be resolved if the emitting matter is moving relativistically toward the observer. In this case the relative angle at which the photons collide must be less than the inverse of the bulk Lorentz factor, $1/\Gamma$, to effectively reduce the threshold energy for e^+e^- pair production (Goodman 1986). One can show that $\Gamma \geq 100$ is required to overcome the compactness problem (Shemi & Piran 1990; Paczyński 1990). This relativistic outflow presumably arises from an initial energy E_0 imparted to a mass $M_0 \ll E_0/c^2$ close to the central engine (see Mészáros 2002 for more details).

Assuming the star is bare[7] in our model, the emitted photons are likely to interact with particles from the accreting material. To enable acceleration to Lorentz factors above 100 the photon energy must be imparted on particles representing on average less than 0.1% of the total matter accreted per episode, since $\Gamma = \eta \dot{m}_{\rm accr} c^2 \Delta t_{\rm accr}/m_{\rm ejec}c^2 = \eta(m_{\rm accr}/m_{\rm ejec})$. In other words, we require most of the infall material to convert to CFL matter with only a small portion of it to be ejected. This seems not unreasonable, as most of the accreted particles will instantly deconfine to quark matter on contact with the star's surface (see, e.g., Weber 2005).

The amount of mass ejected will vary from one episode to another, leading to a spread in the Lorentz factor distribution as already indicated in Figures 3–5. A fast loaded fireball that was injected after a slower one will eventually catch up and collide, converting some of the kinetic energy of the shells to thermal energy. This is reminiscent of the popular internal-shock model

[7] It has been suggested that the plausible surface depletion of *s* quarks induces a Coulomb barrier allowing the presence of a crust (Usov 2004). Nevertheless, a crust should be blown away by the extreme radiation pressure induced by the extreme temperature (tens of mega–electron volts) of the star immediately following its birth and during its early history (e.g., Woosley & Baron 1992). We thus assume that the star is bare for most of the bursting era, during which the high temperatures are maintained by the infalling disk material.

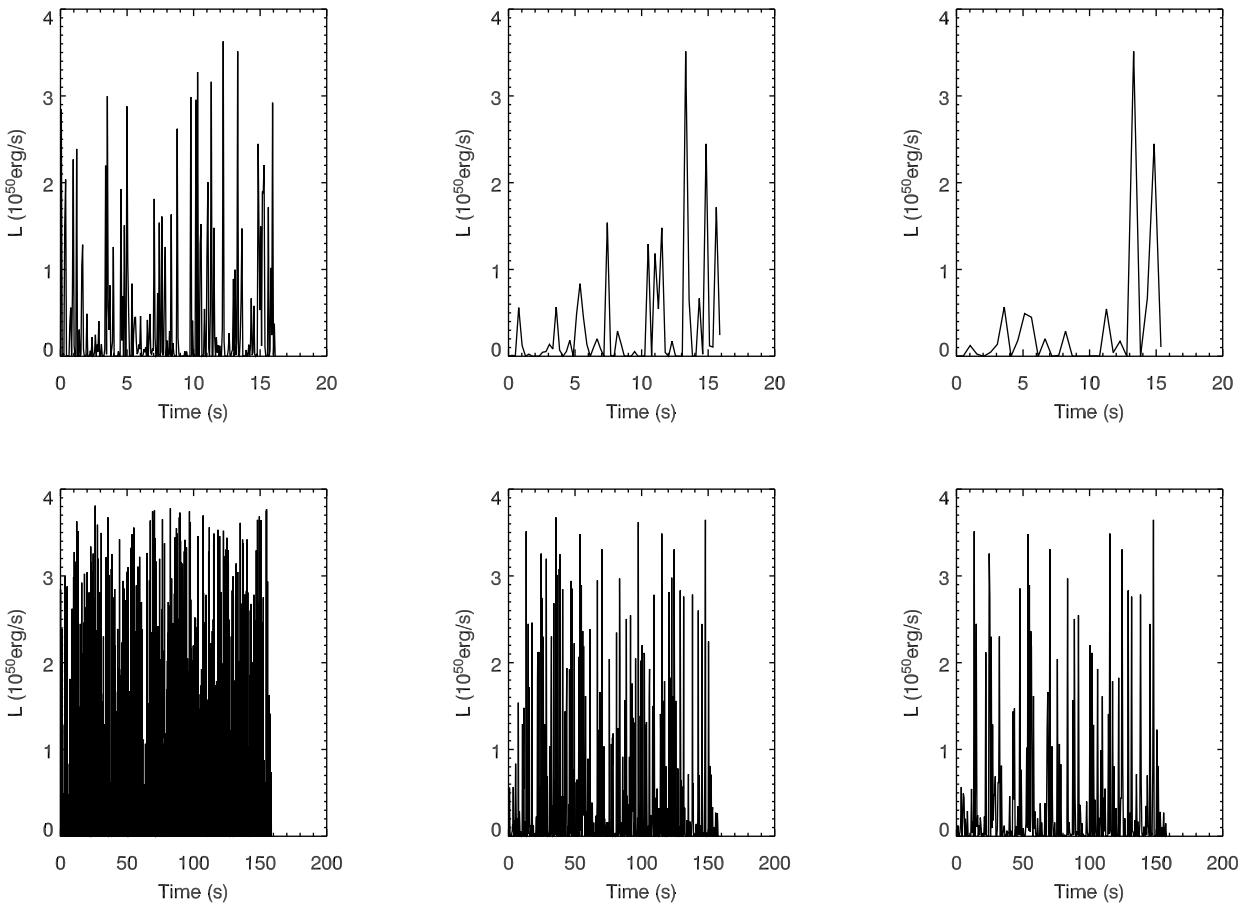

FIG. 4.—Same as Fig. 3 but for $T_{\max} = 20$ MeV. More sample light curves can be found at http://www.capca.ucalgary.ca/.

for GRBs (see, e.g., Kobayashi et al. 1997; Piran 2005) in which a succession of relativistic shells collide and release the shock energy via synchrotron emission and inverse Compton scattering.

The intricate details of the accretion-ejection cycles are beyond the scope of this paper. Qualitatively, taking into account the star-disk magnetic field, we expect accretion to be channeled toward the polar regions as illustrated in Figure 6. A refined scenario could further include hot bursting spots on the surface of the CFL star emitting γ-rays; the outgoing photons interact with the particles from the accreting matter ejecting part of it. Thus, in our model, the loaded fireballs emanate mostly from the polar regions with collimation reinforced by the magnetic field (e.g., Fendt & Ouyed 2004). When a hot spot cools below T_a, further accretion is triggered, leading to another photon-bursting spot on the star as pictured in Figure 6. The time delay between two successive spots is related to the randomness in the accretion (reheating) and the cooling timescales as described in § 3.1. This process continues until E_T is consumed, which in some cases can support up to hundreds of episodes (subjets), as in Figure 5.

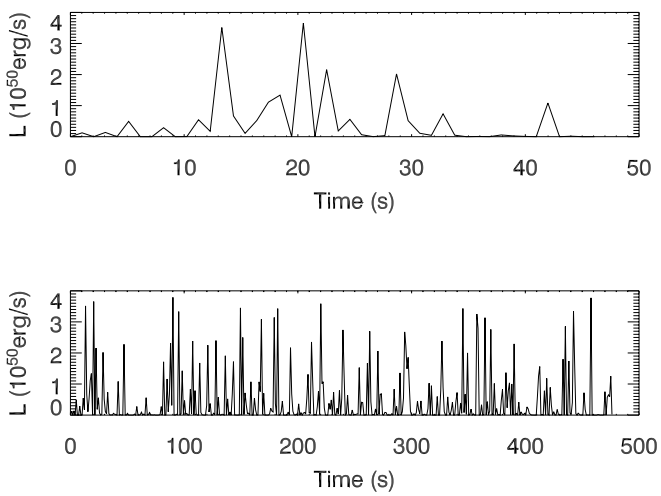

FIG. 5.—GRB emission spectra vs. time for a CFL star with accretion disk of mass 0.01 $M_\odot$ (or $E_T = 0.001 M_\odot c^2$; *top*) and 0.1 $M_\odot$ (or $E_T = 0.01 M_\odot c^2$; *bottom*), with $T_{\max} = 15$ MeV and a time resolution of 1024 ms. More examples can be found at http://www.capca.ucalgary.ca/.

3.5. *Formation Scenarios and Sites*

In scenarios for the formation of CFL stars massive progenitors are naturally favored, since they are more likely to lead to compact remnants with high enough densities in the core for a (phase) transition to quark matter to occur. This is in line with afterglow observations that have provided several hints that some GRBs are associated with massive star progenitors (Galama et al. 1998; van Paradijs 1999). If the quark star forms immediately following a supernova (SN) explosion of a massive progenitor, a thick disk ($M_{\rm disk} > 0.1\ M_\odot$) is expected to form from fallback material. The faster fireballs from the CFL star will catch up with the preceding SN shell and energize it. In fact, the energetic subjets from the CFL star are capable of destroying the original symmetry of the expanding SN shell. Another possibility involving massive progenitors is that of a collapsar-like event (Woosley 1993) in which a quark star is formed instead of a black

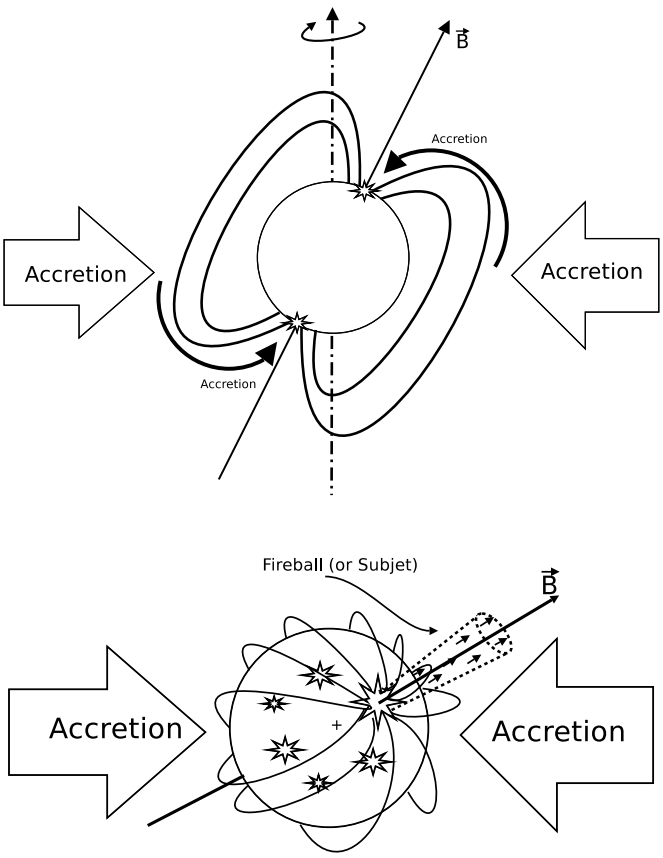

FIG. 6.—Illustration of the intermittent accretion-ejection mechanism in our model. The top panel shows the disk material channeled by the magnetic field toward the polar regions, reheating the surface temperature to $T_{\rm peak}$ (*flashy spots*). When $T_{\rm peak} > T_a$, a photon burst is triggered, ejecting particles from the accreting material. From a viewpoint along the polar axis (*bottom, plus sign*), the multiple flashes on the surface of the star illustrate the locations of previous bursts (or ejections) induced by previous accretion episodes. The spatial spread of these flashes portrays the randomness in the accretion and cooling timescales.

hole. In this scenario as well, one would expect thick and massive disks to form around the star.

The hadron-quark transition may also happen long after the SN explosion, as in the quark-nova model in which a neutron star (originally formed from a massive progenitor) can reach quark-matter densities through accretion from a companion or due to spin down (Ouyed et al. 2002, 2004). In some cases, the phase transition may take tens of millions of years to occur. During the explosion, up to 0.01 $M_\odot$ of material can be ejected (Keränen et al. 2005), which later turns into a hyperaccreting disk (Keränen & Ouyed 2003).

3.6. *Bimodality: Short- and Long-Duration GRBs*

The durations of GRBs observed by the Burst and Transient Source Experiment (BATSE) show a bimodal distribution, which has led to a classification of GRBs into short (with $t_{90} < 2$ s, where t_{90} is the decay time to 10% intensity) and long ($t_{90} > 2$ s; Kouveliotou et al. 1993; McBreen et al. 1994). It has been suggested that different underlying engines are operative, the short ones being related to binary neutron star mergers and the long ones to the collapse of massive stars (see Mészáros 2002 and references therein). However, recent comparisons of short GRBs' light curves to the first few seconds in those of long GRBs indicate that the two classes could be similar (e.g., Nakar & Piran 2002; Ghirlanda et al. 2004).

As noted in § 3.1, our model provides a kind of self-similar behavior in which the variability in the first few seconds of a long-duration GRB (thick disk) is reminiscent of that of a short GRB (thin disk), both driven by the same engine. As for the observed bimodality, it is possible that the formation scenarios discussed in § 3.5 (namely, collapsar-like events and quark-nova explosions) lead to two distinct classes of accretion disk (thick with $M_{\rm disk} > 0.01\ M_\odot$ and thin with $M_{\rm disk} < 0.01\ M_\odot$) surrounding the CFL star.

Interestingly, it has been argued recently in the literature that the bimodality in GRB duration originates from discrete emission regions (subjets) in the GRB jet (Toma et al. 2005 and references therein). In this model the multiplicity of the subjets (n_s) along a line of sight differentiates between short GRBs ($n_s \sim 1$) and long GRBs ($n_s \gg 1$). Many subjets have to be randomly launched by the central engine for the model to work. This bears a close resemblance to the picture that we develop in this paper (cf. Fig. 5) and warrants more detailed studies of accretion-ejection within our model.

4. CONCLUSION

We have studied consequences of previously calculated photon (γ-ray) emission mechanisms in CFL matter for the early cooling of CFL stars. Based on the notion that pertinent emissivities essentially saturate the blackbody limit for temperatures $T \simeq 10$–30 MeV (due to underlying processes involving the Goldstone bosons of CFL matter), we have solved a diffusion equation and found that each photon burst can release an average energy of $\sim 10^{49}$ ergs during a fraction of a millisecond. We have suggested a schematic model within which the time variability and the long activity (up to hundreds of seconds) of a GRB engine is driven by a surrounding hyperaccreting disk resulting from the formation process of a CFL star. This model reproduces several features of observed GRB spectra.

In our simplified picture we assume that photons and neutrinos are emitted at the same temperature (see § 3.4 in VRO04 for a discussion). This certainly is far from a realistic situation in which temperature gradients would be present and the neutrinosphere would be buried deeper in the star at hotter temperatures than the photosphere. In this case neutrinos would dominate the cooling, leading to timescales shorter than the 0.1 ms range we found when only photons are at play. This is of particular importance in the early stages immediately following the formation of the star. On longer timescales and within the GRB context, the reheating mechanism (induced by the infalling accretion disk material) affects mostly the surface layers and thus specifically the photosphere region. A decoupling between the photosphere and the neutrinosphere is to be expected, justifying the neglect of neutrino cooling in the subsequent photon bursts/episodes.

For a more quantitative description of the complex energetics and dynamics involved in our model, advanced numerical simulations should be performed that account for general relativistic effects, as well as for the star-disk magnetic field. Such studies will be similar to what has been done in the case of black hole accretion disk systems (De Villiers et al. 2005), with the black hole replaced by a CFL star.

The research of R. O. is supported by grants from the Natural Science and Engineering Research Council of Canada (NSERC) and the Alberta Ingenuity Fund (AIF), and the research of R. R. is supported in part by a US National Science Foundation CAREER award under grant PHY 04-49489.

REFERENCES

Alcock, C., Farhi, E., & Olinto, A. 1986, ApJ, 310, 261
Alford, M., Bowers, J. A., & Rajagopal, K. 2001, Phys. Rev. D, 63, 074016
Alford, M., & Rajagopal, K. 2002, J. High Energy Phys., 6, 31
Alford, M., Rajagopal, K., & Wilczek, F. 1998, Phys. Lett. B, 422, 247
———. 1999, Nucl. Phys. B, 537, 443
Alford, M., & Reddy, S. 2003, Phys. Rev. D, 67, 074024
Buballa, M., Neuman, F., Oertel, M., & Shovkovy, I. 2004, Phys. Lett. B, 595, 36
Chmaj, T., Haensel, P., & Slomiński, W. 1991, Nucl. Phys. B Proc. Suppl., 24, 40
De Villiers, J. P., Staff, J., & Ouyed, R. 2005, preprint (astro-ph/0502225)
Fendt, C., & Ouyed, R. 2004, ApJ, 608, 378
Frank, J., King, R., & Raine, D. J. 1992, Accretion Power in Astrophysics (Cambridge: Cambridge Univ. Press)
Frolov, V. P., & Lee, H. K. 2005, Phys. Rev. D, 71, 044002
Galama, T., et al. 1998, Nature, 395, 670
Ghirlanda, G., Ghisellini, G., & Celotti, A. 2004, A&A, 422, L55
Glendenning, N. K. 1997, Compact Stars (New York: Springer)
Goodman, J. 1986, ApJ, 308, L47
Jaikumar, P., Prakash, M., & Schäfer, T. 2002, Phys. Rev. D, 66, 063003
Keränen, P., & Ouyed, R. 2003, A&A, 407, L51
Keränen, P., Ouyed, R., & Jaikumar, P. 2005, ApJ, 618, 485
Kobayashi, S., Piran, T., & Sari, R. 1997, ApJ, 490, 92
Kouveliotou, C., Meegan, C. A., Fishman, G. J., Bhat, N. P., Briggs, M. S., Koshut, T. M., Paciesas, W. S., & Pendleton, G. N. 1993, ApJ, 413, L101
Lugones, G., & Horvath, J. E. 2002, Phys. Rev. D, 66, 074017
McBreen, B., Hurley, K. J., Long, R., & Metcalfe, L. 1994, MNRAS, 271, 662
Mészáros, P. 2002, ARA&A, 40, 137
Nakar, E., & Piran, T. 2002, MNRAS, 330, 920
Ouyed, R., Dey, J., & Dey, M. 2002, A&A, 390, L39
Ouyed, R., Elgarøy, Ø., Dahle, H., & Keränen, P. 2004, A&A, 420, 1025
Ouyed, R., & Sannino, F. 2001, Phys. Lett. B, 511, 66
———. 2002, A&A, 387, 725
Paczyński, B. 1990, ApJ, 363, 218
Page, D., & Usov, V. V. 2002, Phys. Rev. Lett., 89, 131101
Piran, T. 2000, Phys. Rep., 333, 529
———. 2005, Rev. Mod. Phys., 76, 1143
Popham, R., Woosley, S. E., & Fryer, C. 1999, ApJ, 518, 356
Rajagopal, K., & Wilczek, F. 2001, in At the Frontier of Particle Physics: Handbook of QCD, Vol. 3, ed. B. L. Ioffe & M. A. Shifman (Singapore: World Scientific), 2061
Rapp, R., Schäfer, T., Shuryak, E. V., & Velkovsky, M. 1998, Phys. Rev. Lett., 81, 53
Rapp, R., Shuryak, E. V., & Zahed, I. 2001, Phys. Rev. D, 63, 034008
Reddy, S., Sadzikowski, M., & Tachibana, M. 2003, Nucl. Phys. A, 714, 337
Ruderman, M. 1975, Ann. NY Acad. Sci., 262, 164
Shemi, A., & Piran, T. 1990, ApJ, 365, L55
Shovkovy, I. A., & Ellis, P. J. 2002, Phys. Rev. C, 66, 015802
Toma, K., Yamazaki, R., & Nakamura, T. 2005, ApJ, 620, 835
Usov, V. V. 2001, ApJ, 550, L179
———. 2004, Phys. Rev. D, 70, 067301
van Paradijs, J. 1999, Science, 286, 693
Vogt, C., Rapp, R., & Ouyed, R. 2004, Nucl. Phys. A, 735, 543 (VRO04)
Weber, F. 2005, Prog. Part. Nucl. Phys., 54, 193
Woosley, S. E. 1993, ApJ, 405, 273
Woosley, S. E., & Baron, E. 1992, ApJ, 391, 228